

Study of p_T -differential radial flow in blast-wave model

Swati Saha,^{1, 2, *} Ranbir Singh,^{1, 2, †} and Bedangadas Mohanty^{1, 2, ‡}

¹*School of Physical Sciences, National Institute of Science Education and Research, Jatni 752050, Odisha, India*

²*Homi Bhabha National Institute, Training School Complex,
Anushaktinagar, Mumbai 400094, Maharashtra, India*

The transverse momentum-differential radial flow observable $v_0(p_T)$, recently proposed and measured by the ATLAS and ALICE collaborations, provides a novel tool to probe radial expansion dynamics in high-energy heavy-ion collisions. In this work, we conduct a detailed study of $v_0(p_T)$ using a blast-wave model that incorporates hydrodynamic-like expansion and thermal emission. We introduce event-by-event fluctuations in the transverse expansion velocity and kinetic freeze-out temperature using Gaussian probability distributions. Our results show that increasing the mean expansion velocity leads to a clear mass ordering in $v_0(p_T)$, while fluctuations in both expansion velocity and freeze-out temperature significantly enhance the magnitude of $v_0(p_T)$, particularly at higher p_T . We fit blast-wave model calculations for identified hadrons (π , K, and p) to recent ALICE data from Pb-Pb collisions at $\sqrt{s_{NN}} = 5.02$ TeV using a Bayesian parameter estimation framework. The extracted mean transverse expansion velocity decreases, while the kinetic freeze-out temperature increases, from central to peripheral collisions. Additionally, the freeze-out temperatures inferred from $v_0(p_T)$ are systematically higher than those obtained from conventional p_T -spectra fits, likely due to the reduced sensitivity of $v_0(p_T)$ to resonance decay contributions.

I. INTRODUCTION

Heavy-ion collisions at the Large Hadron Collider (LHC) and the Relativistic Heavy Ion Collider (RHIC) create extreme conditions in which quarks and gluons become deconfined, forming a hot, dense medium known as the quark-gluon plasma (QGP) [1–3]. As the QGP evolves, strong pressure gradients drive its collective expansion, which is well described by relativistic hydrodynamics [4]. This expansion gives rise to two distinct types of collective motion: anisotropic flow, which reflects momentum anisotropies originating from the initial geometric asymmetries in the collision zone, and radial flow, which corresponds to the isotropic outward push of particles resulting from the system's overall pressure buildup [5–8].

While anisotropic flow has been extensively studied through azimuthal correlations among final-state particles [9–15], investigations of radial flow have been comparatively limited. Recent progress has been made through studies of mean transverse momentum fluctuations [16–21].

Radial flow, associated with the isotropic expansion of the system, is traditionally studied via transverse momentum (p_T) spectra, using simultaneous fits to the distributions of pions, kaons, and protons within the framework of the Boltzmann-Gibbs blast-wave model [22–24]. However, this approach provides only a single value of the radial flow parameter for a given centrality class and does not capture its p_T -dependent behavior.

The recently introduced observable $v_0(p_T)$ enables a p_T -differential study of radial flow by capturing long-

range transverse momentum correlations while effectively suppressing short-range nonflow effects through the use of a pseudorapidity gap [25, 26]. Defined via a normalized covariance between the event-wise mean p_T and the particle yield in p_T bins, $v_0(p_T)$ offers a novel probe of collective dynamics in the QGP. Measurements by both the ALICE and ATLAS collaborations for inclusive charged particles in Pb-Pb collisions at $\sqrt{s_{NN}} = 5.02$ TeV have demonstrated its sensitivity to key medium properties such as bulk viscosity and the QCD equation of state [27, 28]. Recent studies employing full (3+1)D hydrodynamic simulations using the MUSIC framework have shown that $v_0(p_T)$ for identified particles exhibits a clear mass ordering at low p_T . This behavior, attributed to collective expansion dynamics, is analogous to the well-known mass ordering observed in the elliptic flow coefficient $v_2(p_T)$ [25, 26]. In such models, the magnitude and shape of $v_0(p_T)$ are found to be sensitive to initial-state fluctuations, transport coefficients (such as bulk viscosity), and freeze-out conditions. ALICE measurements confirm the mass-dependent behavior at low p_T and also reveal baryon-meson separation at intermediate p_T [27]. These observations establish $v_0(p_T)$ as a sensitive tool for studying collective expansion, providing complementary insights beyond those available from conventional flow observables.

In this work, we analyze $v_0(p_T)$ for pions, kaons, and protons within the theoretical framework of the Boltzmann-Gibbs blast-wave model [22] for Pb-Pb collisions at $\sqrt{s_{NN}} = 5.02$ TeV. The blast-wave model provides a simplified, hydrodynamically motivated description of the kinetic freeze-out stage, in which a locally thermalized medium undergoes collective radial expansion. In this framework, the transverse momentum spectra of final-state particles are governed primarily by two parameters: the radial flow velocity, which reflects the collective expansion strength, and the kinetic freeze-out

* swati.saha@niser.ac.in

† ranbir.singh@niser.ac.in

‡ bedanga@niser.ac.in

temperature, which characterizes the thermal conditions at decoupling. This study establishes a connection between the traditional extraction of radial flow and freeze-out temperature via hadron p_T spectra and the corresponding results derived from $v_0(p_T)$. Additionally, we aim to disentangle the contributions of thermal motion and collective flow to the behavior of $v_0(p_T)$.

The paper is organized as follows: Section II defines the $v_0(p_T)$ observable and outlines the analysis methodology; Section III presents the results of the blast-wave model calculations and compares them with ALICE measurements; and Section IV summarizes the main findings and their implications.

II. OBSERVABLE AND METHODOLOGY

We follow the definition of $v_0(p_T)$ from Refs. [25, 26], which characterizes event-by-event fluctuations in the transverse momentum spectra:

$$v_0(p_T) = \frac{\langle \delta f(p_T) \delta[p_T] \rangle}{\langle f(p_T) \rangle \sigma([p_T])}. \quad (1)$$

Here, $[p_T]$ denotes the event-by-event mean transverse momentum of charged particles, and $f(p_T)$ is the normalized transverse momentum distribution, related to the event-by-event p_T spectra by

$$f(p_T) = \frac{N(p_T)}{\int N(p_T) dp_T}. \quad (2)$$

The quantities $\delta f(p_T)$ and $\delta[p_T]$, which quantify the fluctuations of $f(p_T)$ and $[p_T]$ about their event averages, are given by

$$\delta f(p_T) = f(p_T) - \langle f(p_T) \rangle, \quad \delta[p_T] = [p_T] - \langle [p_T] \rangle. \quad (3)$$

In the Boltzmann-Gibbs blast-wave model, particle production is described by

$$E \frac{d^3 N}{dp^3} \propto \int_0^R m_T I_0 \left(\frac{p_T \sinh(\rho)}{T_{\text{kin}}} \right) K_1 \left(\frac{m_T \cosh(\rho)}{T_{\text{kin}}} \right) r dr, \quad (4)$$

where m_T is the transverse mass, defined as $m_T = \sqrt{m^2 + p_T^2}$, T_{kin} is the temperature at kinetic freeze-out, I_0 and K_1 are modified Bessel functions, and r is the radial distance in the transverse plane. Equation 4 is used to generate event-by-event p_T spectra for estimating $v_0(p_T)$. The radial expansion velocity profile ρ is parametrized as

$$\rho = \tanh^{-1} \beta_T(r) = \tanh^{-1} \left[\left(\frac{r}{R} \right)^n \beta_s \right], \quad (5)$$

where R is the fireball radius, $\beta_T(r)$ is the radial velocity, and β_s is the transverse velocity at the fireball

surface. The mean radial expansion velocity $\langle \beta_T \rangle$ is related to β_s by

$$\langle \beta_T \rangle = \frac{\int_0^R \beta_T(r) r dr}{\int_0^R r dr} \implies \beta_s = \langle \beta_T \rangle \left(\frac{n+2}{2} \right). \quad (6)$$

Thus, for a given value of $\langle \beta_T \rangle$, the corresponding β_s can be determined using Eq. 6. The Boltzmann-Gibbs blast-wave function (Eq. 4) is typically used to simultaneously fit the p_T spectra of charged pions, kaons, and protons using a common parameter set, while allowing for separate normalization factors and masses.

The parameter set reported in Ref. [24] is used to generate event-by-event blast-wave spectra, and the averaged spectrum is compared with experimental data in Fig. 1. The spectra are obtained for the 10–20% centrality class using the parameter values $\langle \beta_T \rangle = 0.655$ (yielding $\beta_s = 0.897$), $T_{\text{kin}} = 0.094$ GeV, and $n = 0.739$. The normalization factors are adjusted to match the experimental spectra, ensuring a reliable estimate of the mean p_T for inclusive charged particles.

These generated blast-wave spectra, tuned to reproduce the measured p_T distributions of pions, kaons, and protons, provide a realistic baseline to investigate how event-by-event fluctuations in the radial flow velocity and kinetic freeze-out temperature influence the behavior of $v_0(p_T)$. While the mean values of these parameters determine the shape of the average spectra, their fluctuations manifest in $v_0(p_T)$.

To systematically quantify these effects, we introduce Gaussian fluctuations in β_s and T_{kin} and consider four scenarios in which either the mean or the width of each parameter is varied independently: (i) varying the mean of β_s while keeping its fluctuation width and T_{kin} fixed, (ii) varying the fluctuation width of β_s while keeping its mean and T_{kin} fixed, (iii) varying the mean of T_{kin} while β_s is held constant, and (iv) varying the fluctuation width of T_{kin} while its mean and β_s are kept fixed.

These controlled variations allow us to probe the respective roles of thermal motion and collective flow fluctuations in shaping the structure of $v_0(p_T)$. In the following section, we present the results of our analysis, emphasizing the sensitivity of $v_0(p_T)$ to variations in blast-wave parameters.

III. RESULTS AND DISCUSSION

The effect of varying the surface transverse expansion velocity β_s on the evolution of $v_0(p_T)$ for individual particle species—pions (left), kaons (middle), and protons (right)—is shown in Fig. 2. The results correspond to four different β_s values ranging from 0.697 to 0.927, with a fixed kinetic freeze-out temperature $T_{\text{kin}} = 0.094$ GeV and a fluctuation width of $\sigma(\beta_s) = 0.006$.

For all particle species, the general trend is that $v_0(p_T)$ transitions from negative values at low p_T to positive

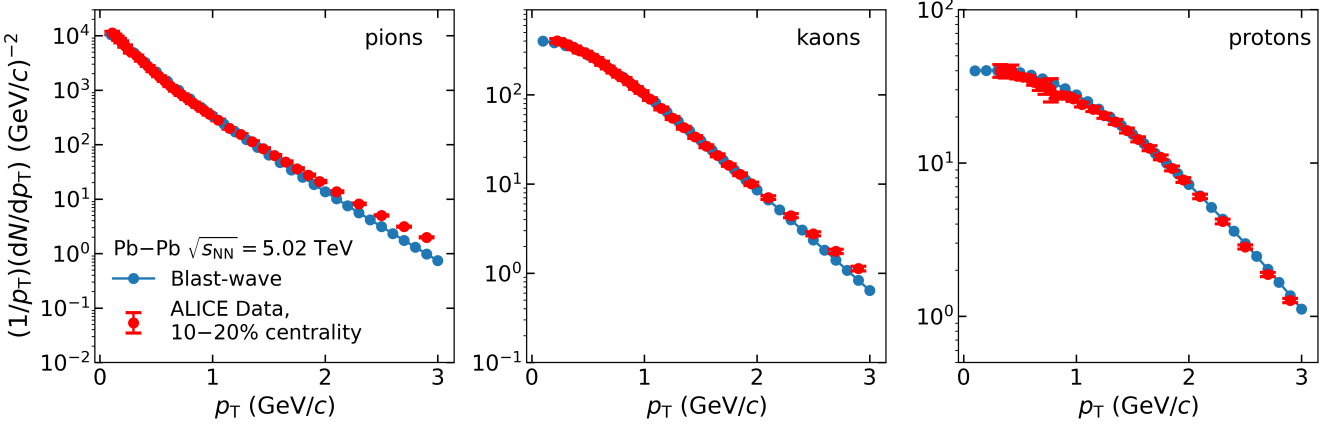


FIG. 1. Transverse momentum spectra of pions (left), kaons (middle), and protons (right) measured in Pb–Pb collisions at $\sqrt{s_{\text{NN}}} = 5.02$ TeV for centrality class 10–20% is compared with blast-wave model generated results using the parameters $\beta_s = 0.897$, $T_{\text{kin}} = 0.094$ GeV, and $n = 0.739$ from Ref. [24].

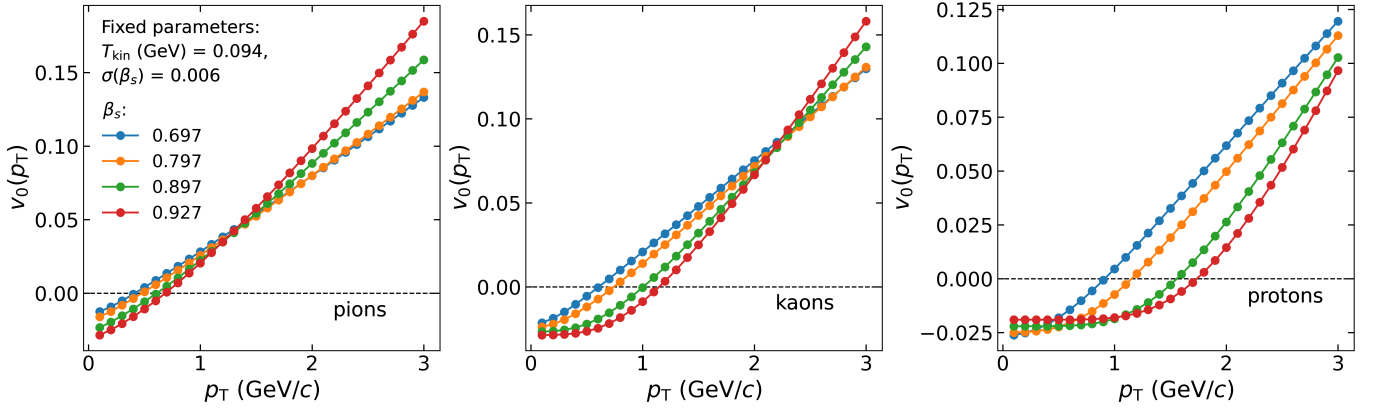


FIG. 2. $v_0(p_T)$ for pions (left), kaons (middle), and protons (right) from the blast-wave model incorporating Gaussian fluctuations in the transverse expansion velocity at the surface. The kinetic freeze-out temperature (T_{kin}) and the fluctuation width of the surface velocity $\sigma(\beta_s)$ are fixed at 0.094 GeV and 0.006, respectively, while the mean surface velocity β_s is varied in the range [0.697, 0.927].

values beyond a threshold transverse momentum, $p_{\text{T,sep}}$. This threshold increases with β_s , indicating that higher expansion velocities shift the onset of positive $v_0(p_T)$ to larger p_T . The increase in $p_{\text{T,sep}}$ with β_s is most significant for protons, followed by kaons and then pions, indicating that stronger radial flow enhances the mass-dependent separation among particle species.

The left panel presents results for pions, where $v_0(p_T)$ increases almost linearly for all β_s . For $p_T < 1.5 \text{ GeV}/c$, higher β_s values lead to a reduction in $v_0(p_T)$, whereas for $p_T > 1.5 \text{ GeV}/c$, increasing β_s results in an enhancement. Similar results for kaons, shown in the middle panel, reveal a more nonlinear dependence on p_T at higher β_s values compared to pions. For $p_T < 2.5 \text{ GeV}/c$, increasing β_s reduces $v_0(p_T)$, following a trend similar to that of pions but with greater non-linearity. The transition point where $v_0(p_T)$ begins to increase with β_s occurs at a higher p_T than for pions. Beyond this point, $v_0(p_T)$

rises more steeply with p_T as β_s increases, although the overall change in magnitude remains modest.

The right panel displays results for protons, which exhibit the strongest nonlinear response to changes in β_s among the three species. At the lowest β_s , $v_0(p_T)$ follows a linear trend with p_T , but as β_s increases, the dependence becomes increasingly nonlinear—more so than for kaons. For $p_T < 0.5 \text{ GeV}/c$, the effect of β_s is minimal, whereas for $p_T > 1 \text{ GeV}/c$, larger β_s leads to a stronger suppression of $v_0(p_T)$, consistent with the trends observed for pions and kaons.

Figure 3 illustrates the behavior of $v_0(p_T)$ for pions (left), kaons (middle), and protons (right), incorporating Gaussian fluctuations in β_s . The kinetic freeze-out temperature T_{kin} and the mean value of β_s are held constant, while the width of the fluctuations, $\sigma(\beta_s)$, is systematically varied from 0.003 to 0.015. The results indicate a clear dependence of $v_0(p_T)$ on $\sigma(\beta_s)$ for all three particle

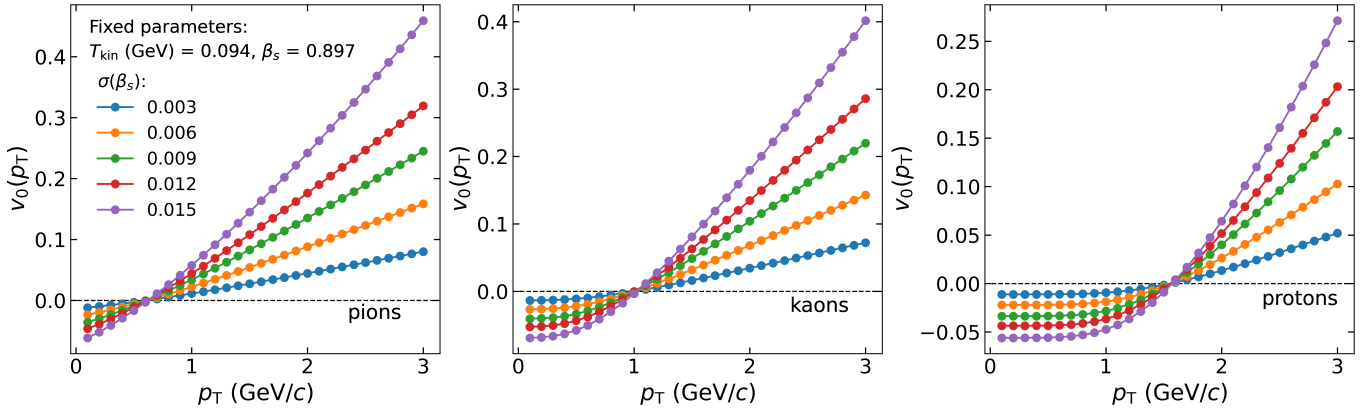


FIG. 3. $v_0(p_T)$ of pions (left), kaons (middle), and protons (right) in blast-wave model for Gaussian-fluctuations of transverse expansion velocity at the surface. The kinetic freeze-out temperature (T_{kin}) and mean value of fluctuations β_s are kept fixed at 0.094 GeV and 0.897, respectively, while the width $\sigma(\beta_s)$ is varied in the range [0.003, 0.015].

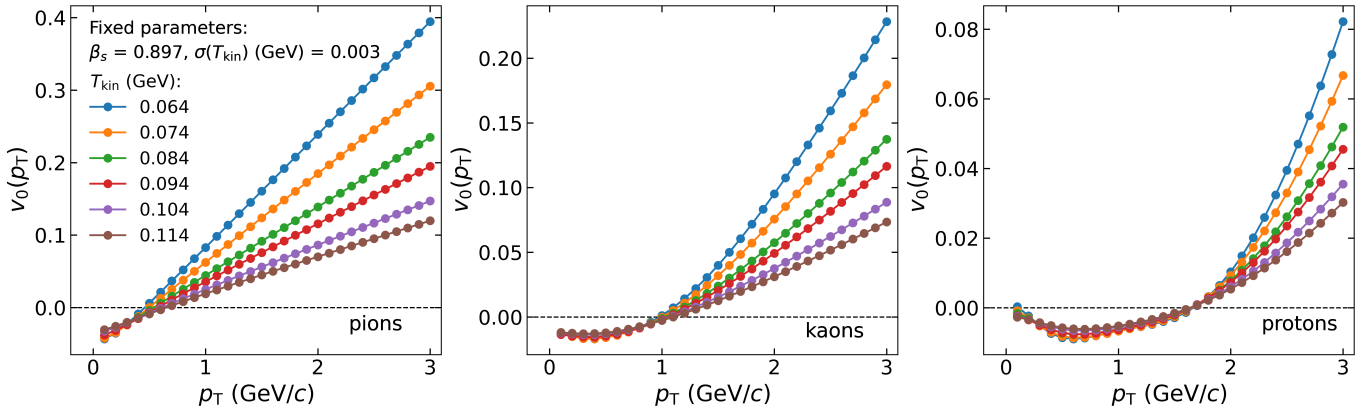


FIG. 4. $v_0(p_T)$ of pions (left), kaons (middle), and protons (right) in blast-wave model for Gaussian-fluctuations of kinetic freeze-out temperature. The transverse expansion velocity at the surface (β_s) and width of fluctuations $\sigma(T_{\text{kin}})$ are kept fixed at 0.897 and 0.003 GeV, respectively, while the mean value T_{kin} is varied in the range [0.064, 0.114] GeV.

species.

Increasing fluctuations in β_s lead to an overall increase in the magnitude of $v_0(p_T)$ both below and above $p_{T,\text{sep}}$. This effect is more significant for $p_T > p_{T,\text{sep}}$ than for $p_T < p_{T,\text{sep}}$ and becomes more pronounced with increasing p_T . Despite the variation in $\sigma(\beta_s)$, the threshold $p_{T,\text{sep}}$ —which marks the transition between low- and high- p_T behavior—remains invariant across all three particle species. The slope of $v_0(p_T)$ at high p_T is steepest for protons, followed by kaons and then pions, suggesting that the impact of β_s fluctuations is stronger for heavier particles. As protons are more massive than kaons and pions, they exhibit greater sensitivity to variations in β_s .

The effect of Gaussian fluctuations in T_{kin} on the magnitude of $v_0(p_T)$ is illustrated in FIG. 4. The values of β_s and the fluctuation width of T_{kin} , $\sigma(T_{\text{kin}})$, are fixed at 0.897 and 0.003 GeV, respectively, while the mean value of T_{kin} is systematically varied. The results for pions (left), kaons (middle), and protons (right) are shown for T_{kin} values ranging from 0.064 GeV to 0.114 GeV.

No significant change in $v_0(p_T)$ is observed below the

corresponding $p_{T,\text{sep}}$ for each particle species. However, for $p_T > p_{T,\text{sep}}$, $v_0(p_T)$ decreases with increasing T_{kin} across all species, with the effect becoming more pronounced at higher p_T . This trend suggests that a higher T_{kin} —corresponding to increased thermal motion—tends to dilute fluctuations in the p_T spectra, thereby reducing $v_0(p_T)$.

Furthermore, the mass hierarchy and separation among particle species in $v_0(p_T)$ remain largely unaffected by variations in T_{kin} , in contrast to the stronger sensitivity observed with changes in β_s , which more directly influence these effects.

FIGURE 5 illustrates the dependence of $v_0(p_T)$ on p_T for pions (left), kaons (middle), and protons (right). The primary focus of this figure is to examine the effect of varying the width of Gaussian fluctuations in T_{kin} . The fluctuation width, $\sigma(T_{\text{kin}})$, is varied from 0.003 GeV to 0.01 GeV, while β_s is fixed at 0.897 and the mean value of T_{kin} is held constant at 0.094 GeV.

The results reveal a strong dependence of $v_0(p_T)$ on $\sigma(T_{\text{kin}})$ across all three particle species, resembling the

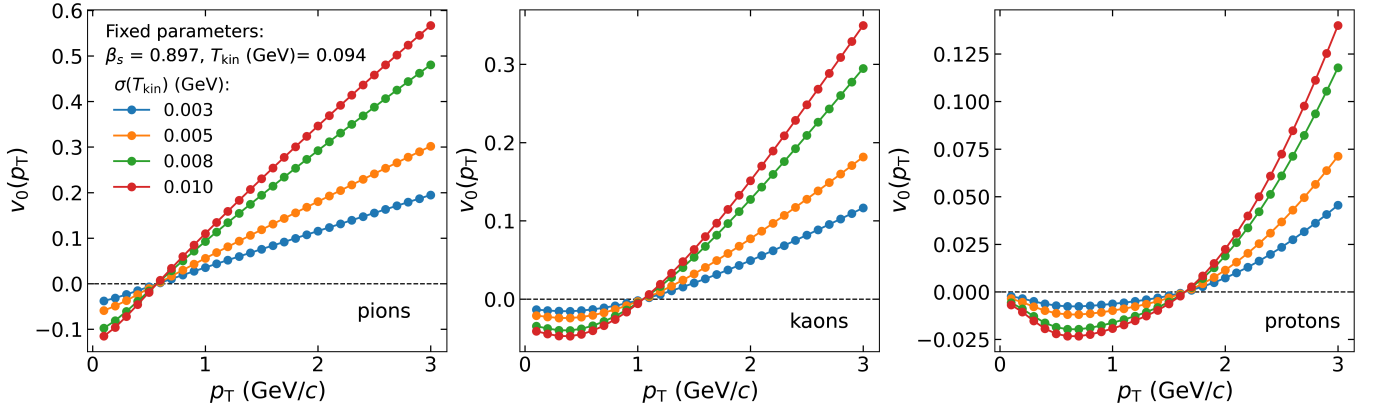


FIG. 5. $v_0(p_T)$ of pions (left), kaons (middle), and protons (right) in blast-wave model for Gaussian-fluctuations of kinetic freeze-out temperature. The transverse expansion velocity at the surface (β_s) and mean value of fluctuations T_{kin} are kept fixed at 0.897 and 0.094 GeV, respectively, while the width $\sigma(T_{\text{kin}})$ is varied in the range [0.003, 0.010] GeV.

TABLE I. Summary of the key findings from the blast-wave model investigation of $v_0(p_T)$ by the variation of mean values for transverse expansion velocity (β_s), kinetic freeze-out temperature (T_{kin}), and their fluctuations ($\sigma(\beta_s)$ and $\sigma(T_{\text{kin}})$).

Parameter increased	Observed Trends
β_s (mean)	<ul style="list-style-type: none"> - Increases the difference in $v_0(p_T)$ between particle species - $v_0(p_T)$ increases at high p_T but decreases at low p_T - $p_{T,\text{sep}}$ shifts to higher values, effect more pronounced for heavier particles
$\sigma(\beta_s)$	<ul style="list-style-type: none"> - Enhances $v_0(p_T)$ across the whole p_T range - No change in the position of $p_{T,\text{sep}}$
T_{kin} (mean)	<ul style="list-style-type: none"> - No change in the difference in $v_0(p_T)$ between particle species - $v_0(p_T)$ decreases above $p_{T,\text{sep}}$, no change in the magnitude below $p_{T,\text{sep}}$ - No change in the position of $p_{T,\text{sep}}$
$\sigma(T_{\text{kin}})$	<ul style="list-style-type: none"> - Increases $v_0(p_T)$, particularly at high p_T - No change in the position of $p_{T,\text{sep}}$

trends observed for $\sigma(\beta_s)$ in Fig. 3. As fluctuations in T_{kin} increase, the magnitude of $v_0(p_T)$ increases both below and above $p_{T,\text{sep}}$. This effect is more pronounced at higher p_T , particularly for $p_T > p_{T,\text{sep}}$, where the rise in $v_0(p_T)$ becomes steeper. Notably, the slope of $v_0(p_T)$ at high p_T is steepest for protons, followed by kaons and pions, indicating a stronger sensitivity of heavier particles to fluctuations in T_{kin} .

Table I summarizes how collective expansion and thermal motion shape the structure of $v_0(p_T)$ within the blast-wave model by varying β_s , T_{kin} , and their fluctuations. Although the blast-wave framework does not incorporate initial-state geometry or the full dynamical evolution of the collision, it captures the essential physics underlying mass ordering and the general behavior of $v_0(p_T)$. In particular, the model demonstrates how radial flow and its event-by-event fluctuations, along with variations in freeze-out temperature, govern the p_T -differential behavior of $v_0(p_T)$ observed across different particle species.

The qualitative agreement between these results and those from more complex hydrodynamic simulations suggests that the blast-wave approach serves as a simplified yet effective tool for interpreting $v_0(p_T)$. Incorporating

resonance decay contributions and initial-state geometry effects will be important directions for future work, enabling a more quantitative comparison with full hydrodynamic models.

For the extraction of radial flow parameters, the blast-wave predictions of $v_0(p_T)$ for pions, kaons, and protons are compared to measurements reported by ALICE for the centrality classes 10–20%, 30–40%, and 60–70%. The parameter inference is performed using Bayesian parameter estimation, a rigorous probabilistic framework that combines prior knowledge of the parameters with experimental data to update the probability distributions describing their values. This approach yields a posterior probability distribution for each model parameter via Bayes' theorem.

Markov Chain Monte Carlo (MCMC) methods are employed to efficiently sample the posterior distribution, enabling robust uncertainty quantification and capturing correlations between parameters. The posterior distributions reflect both the information content of the data and the inherent uncertainties, as shown in Fig. 6. Uniform (uninformative) priors are applied over physically motivated ranges for all model parameters, as listed in Table II. These bounds are chosen based on typical freeze-

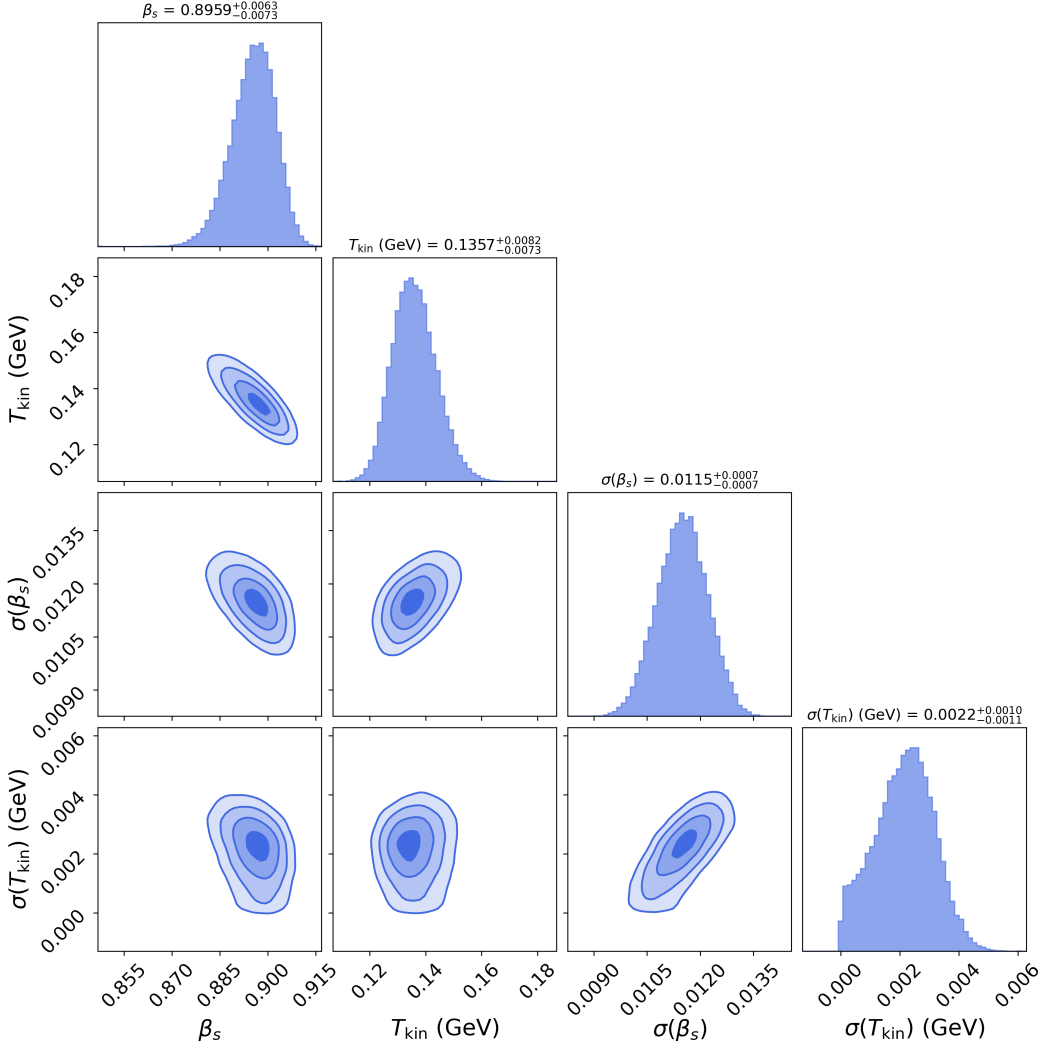


FIG. 6. The posterior distributions and parameter correlations for β_s , T_{kin} , $\sigma(\beta_s)$, and $\sigma(T_{\text{kin}})$ using $v_0(p_{\text{T}})$ measurements of pions, kaons, and protons for centrality classes 10–20% [27]. The diagonal panels display the marginalized probability distributions of individual parameters, while the off-diagonal panels show the 2D joint distributions with contour levels indicating confidence regions. The plot suggests correlations between some parameters, highlighting the uncertainties in their estimations.

out conditions inferred from previous heavy-ion collision studies at LHC energies. A modest extension of these prior ranges (e.g., by $\pm 10\text{--}20\%$) was tested and found not to significantly alter the posterior distributions, confirming that the results are primarily data-driven.

A single set of model parameters is used to jointly describe the $v_0(p_{\text{T}})$ distributions of all three particle species within each centrality class. In the fitting procedure, the chi-squared (χ^2) statistic is computed as the deviation between the blast-wave model predictions and the experimental data at the same p_{T} intervals used for fitting the p_{T} spectra in Ref. [24]. The p_{T} intervals are 0.5–1 GeV/ c , 0.2–1.5 GeV/ c , and 0.3–3 GeV/ c for charged pions, kaons, and protons, respectively.

For the 10–20% centrality interval, the Bayesian analysis yields the following median parameter estimates

TABLE II. Uniform prior ranges used for the blast-wave model parameters in the Bayesian analysis of $v_0(p_{\text{T}})$ for pions, kaons, and protons.

Model parameter	Prior ranges
β_s	[0.60, 0.92]
T_{kin} (GeV)	[0.08, 0.35]
$\sigma(\beta_s)$	[0.001, 0.06]
$\sigma(T_{\text{kin}})$ (GeV)	[0.0, 0.05]

with their corresponding 68% credible intervals: $\beta_s = 0.8959^{+0.0063}_{-0.0073}$, $T_{\text{kin}} = 0.1357^{+0.0082}_{-0.0073}$ GeV, and their event-by-event fluctuations are found to be $\sigma(\beta_s) = 0.0115^{+0.0007}_{-0.0007}$, and $\sigma(T_{\text{kin}}) = 0.0022^{+0.0010}_{-0.0011}$ GeV. The model predictions of $v_0(p_{\text{T}})$ computed with these best-fit parameters are shown alongside the ALICE experimen-

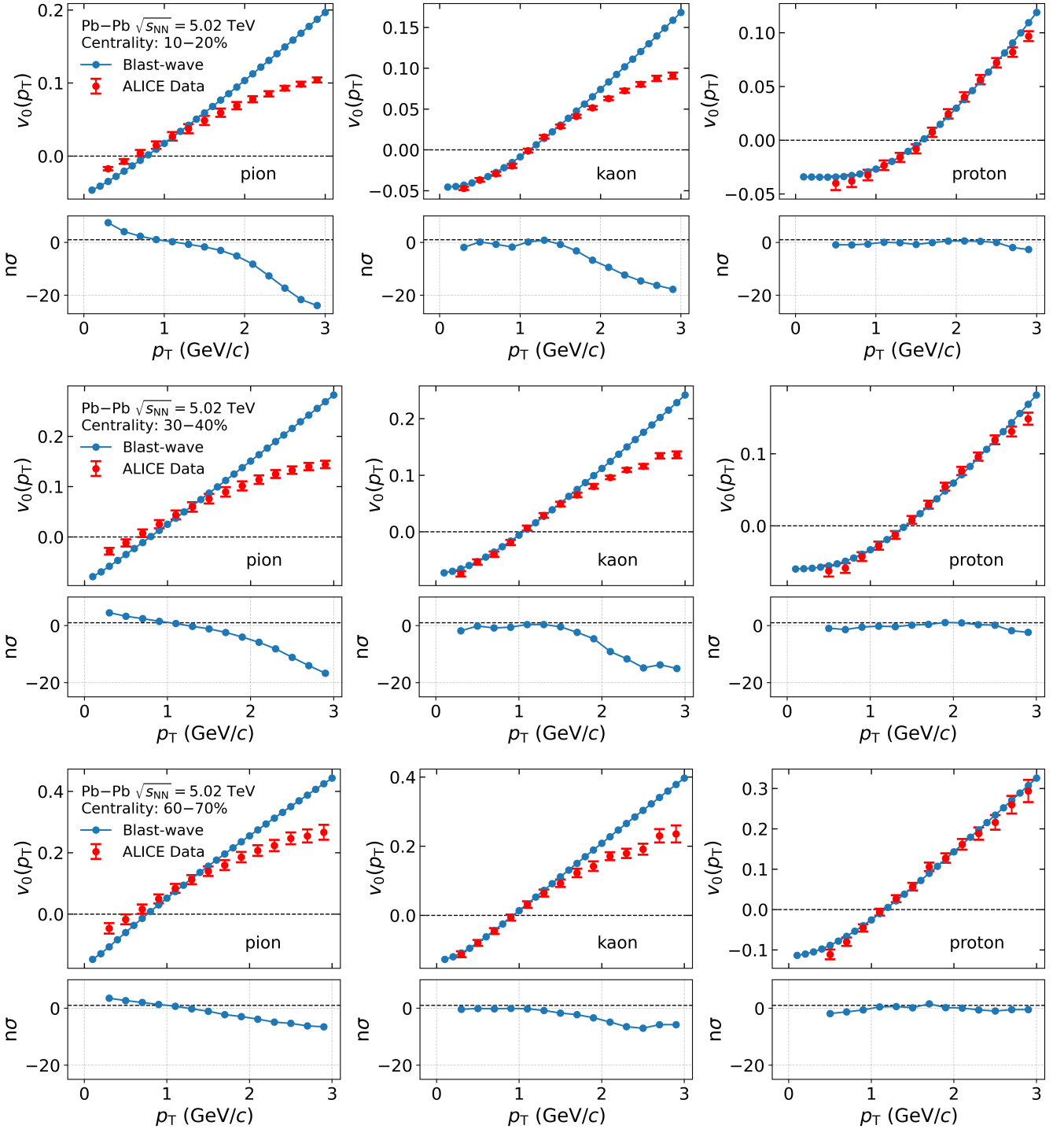


FIG. 7. $v_0(p_T)$ of pions (left), kaons (middle), and protons (right) in Pb–Pb collisions at $\sqrt{s_{\text{NN}}} = 5.02$ TeV for centrality classes 10–20%, 30–40%, and 60–70%. The measurements of ALICE [27] (red marker) are compared to blast-wave predictions obtained with the best-fit parameters. The bottom panels show the residual, $n\sigma = (\text{data} - \text{model})/\sigma_{\text{Data}}$.

tal data in Fig. 7 for three different centrality intervals. The smaller bottom panels in Fig. 7 display the residuals normalized by the total experimental uncertainty, i.e., $(\text{Data}-\text{Model})/\sigma_{\text{Data}}$. A value of zero indicates perfect agreement, while deviations within 2σ suggest con-

sistency between data and model. This comparison in Fig. 7 demonstrates that the blast-wave model with the extracted parameters successfully captures the key features of the data. A very good agreement is noted for

protons, which is followed by kaons and pions.

A detailed summary of the inferred parameters and their uncertainties for all three centrality intervals studied is compiled in Table III. There is a clear decreasing trend in β_s from central to peripheral collisions. For the 10–20% centrality class, β_s is approximately 0.896, indicating strong collective expansion. This value systematically decreases to about 0.842 in the 30–40% class and further to 0.700 in the 60–70% class, reflecting the expected weakening of collective flow in less central collisions.

In contrast, T_{kin} increases from central to peripheral collisions, rising from approximately 0.136 GeV at 10–20% centrality to 0.172 GeV and 0.235 GeV in the 30–40% and 60–70% classes, respectively. This trend is consistent with a scenario in which particles in peripheral collisions decouple earlier at higher temperatures due to the shorter lifetime and smaller system size, whereas in more central collisions the system expands and cools for a longer period before freeze-out.

The event-by-event fluctuations $\sigma(\beta_s)$ and $\sigma(T_{\text{kin}})$ exhibit a pronounced increase from central to peripheral collisions. Specifically, $\sigma(\beta_s)$ rises from approximately 0.012 in 10–20% centrality to 0.021 and 0.046 in the 30–40% and 60–70% classes, respectively, reflecting enhanced variability in the collective expansion strength in smaller systems. Similarly, $\sigma(T_{\text{kin}})$ increases from around 0.002 GeV to 0.006 GeV and 0.020 GeV, indicating more pronounced thermal fluctuations at kinetic decoupling. This escalation of fluctuations in peripheral collisions can be attributed to the reduced system size and shorter lifetime.

Figure 8 compares the values of β_s and T_{kin} extracted in this analysis using $v_0(p_T)$ measurements with those obtained from blast-wave fits to p_T spectra in Ref. [24] (with β_s values derived using Eq. 6). As shown in the left panel, the β_s values from both methods are consistent within uncertainties, with deviations remaining below 2σ . In contrast, the right panel shows significant differences in the extracted T_{kin} values: the temperatures from the $v_0(p_T)$ analysis are systematically higher than those from the p_T spectra.

A key reason for this discrepancy lies in the differing sensitivity of the two observables to resonance decays. The p_T spectra include contributions from short-lived resonances that decay into lighter hadrons, particularly at low p_T . These decay products tend to broaden and soften the spectra, leading to a lower apparent freeze-out temperature when fitted with a blast-wave model. In contrast, $v_0(p_T)$ is extracted from two-particle correlation functions using a pseudorapidity gap, which suppresses short-range correlations, including those from resonance decays. Since resonance decay pairs typically emerge close in angle and rapidity, their contribution to $v_0(p_T)$ is significantly reduced. As a result, the reduced influence of resonances in $v_0(p_T)$ may offer a different perspective and a more direct probe of the thermal conditions at kinetic freeze-out.

IV. SUMMARY AND OUTLOOK

We have investigated the transverse momentum dependence of the radial flow observable $v_0(p_T)$, which characterizes the isotropic expansion of the hot and dense medium created in high-energy heavy-ion collisions. Our analysis focuses on identified particles—pions, kaons, and protons—using a blast-wave model that incorporates Gaussian event-by-event fluctuations in the transverse expansion velocity and kinetic freeze-out temperature.

The model qualitatively reproduces key features of the $v_0(p_T)$ distributions observed in recent ALICE data. Furthermore, using this model, we provide insight into how (a) radial flow, (b) radial flow fluctuations, (c) kinetic freeze-out temperature, and (d) temperature fluctuations affect the p_T dependence of the observable. For smaller mean values of β_s , $v_0(p_T)$ shows little mass dependence; however, increasing β_s leads to a clear mass ordering, reflecting stronger radial flow. The $v_0(p_T)$ transitions from negative values at low p_T to positive values above a species-dependent threshold $p_{T,\text{sep}}$, which shifts to higher p_T with increasing β_s . Fluctuations in β_s and T_{kin} amplify the magnitude of $v_0(p_T)$, particularly at higher p_T , with heavier particles exhibiting greater sensitivity.

Using Bayesian parameter estimation, we extracted blast-wave parameters and their event-by-event fluctuations by fitting $v_0(p_T)$ to ALICE measurements in Pb–Pb collisions at $\sqrt{s_{\text{NN}}} = 5.02$ TeV for three centrality intervals: 10–20%, 30–40%, and 60–70%. The results reveal a systematic decrease in β_s and increase in T_{kin} from central to peripheral collisions, consistent with reduced collective expansion and earlier freeze-out in smaller systems. This general anti-correlation between β_s and T_{kin} has been observed in heavy-ion collisions when these parameters are extracted using hadron p_T spectra. The fluctuation widths $\sigma(\beta_s)$ and $\sigma(T_{\text{kin}})$ also increase toward peripheral collisions, indicating enhanced event-by-event variability.

Model predictions based on the best-fit parameters describe the experimental data well at low p_T , with the strongest agreement observed for protons (over a larger p_T range), followed by kaons and pions. These results provide new insights into the nature of collective expansion and freeze-out dynamics, highlighting the role of flow strength, thermal motion, and their fluctuations in shaping $v_0(p_T)$ across different collision centralities.

An important extension of this work would be to apply $v_0(p_T)$ modeling to smaller systems such as pp and p–Pb collisions. The nature and origin of collectivity in these systems have been under active investigation since the first observation of long-range, near-side correlations in two-particle distributions [29, 30]. Although the blast-wave model can, in principle, be adapted to such systems by constraining the system size and freeze-out conditions, interpreting $v_0(p_T)$ in this context may require incorporating additional physics, such as initial-state momentum correlations or non-equilibrium dynamics, to account for the different underlying mechanisms compared to heavy-

TABLE III. Extracted blast-wave parameters and their event-by-event fluctuation width for different centrality intervals.

Centrality	β_s	T_{kin} (GeV)	$\sigma(\beta_s)$	$\sigma(T_{\text{kin}})$ (GeV)
10–20%	$0.8959^{+0.0063}_{-0.0073}$	$0.1357^{+0.0082}_{-0.0073}$	$0.0115^{+0.0007}_{-0.0007}$	$0.0022^{+0.0010}_{-0.0011}$
30–40%	$0.8420^{+0.0125}_{-0.0142}$	$0.1719^{+0.0117}_{-0.0107}$	$0.0212^{+0.0011}_{-0.0011}$	$0.0065^{+0.0019}_{-0.0021}$
60–70%	$0.7005^{+0.0379}_{-0.0424}$	$0.2346^{+0.0185}_{-0.0183}$	$0.0455^{+0.0046}_{-0.0046}$	$0.0201^{+0.0030}_{-0.0032}$

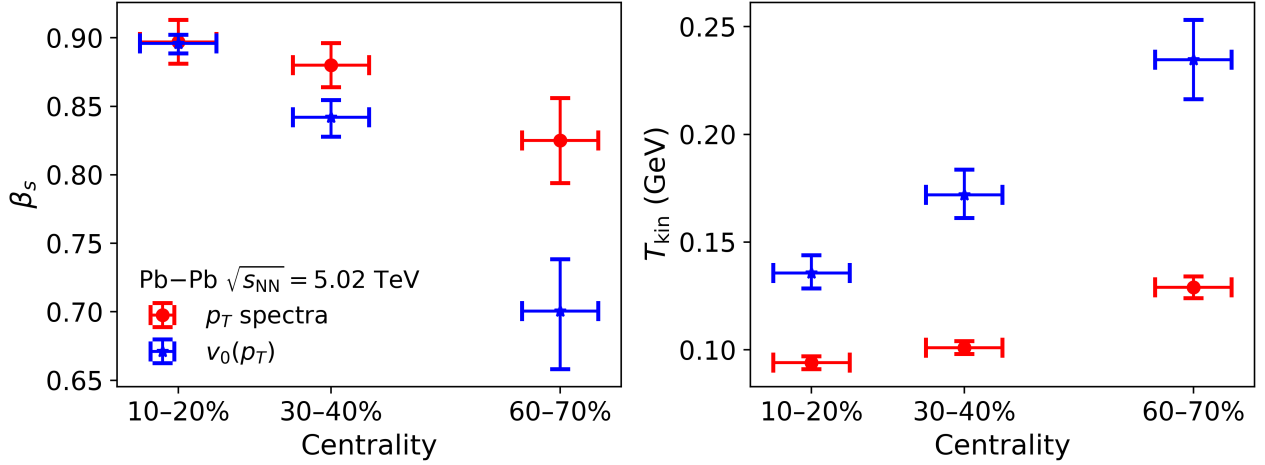


FIG. 8. Comparison of (left) β_s and (right) T_{kin} values obtained in this analysis using $v_0(p_T)$ measurements with those extracted from blast-wave fits to p_T spectra reported in Ref. [24].

ion collisions. Future studies should also consider incorporating event-by-event geometry and system-size fluctuations, which are not included in the current blast-wave implementation but may significantly influence $v_0(p_T)$, especially in small collision systems.

Moreover, at lower collision energies—such as those explored in the RHIC Beam Energy Scan program—the changing balance between thermal pressure and baryon density, along with possible critical fluctuations near the QCD phase transition, may imprint distinct signatures on $v_0(p_T)$. Studying $v_0(p_T)$ systematically across different systems and energies could thus offer new insights into the interplay between radial flow, fluctuations, and

the underlying properties of QCD matter.

ACKNOWLEDGMENTS

This work is supported by the Department of Atomic Energy (DAE), Government of India. We also acknowledge the use of Garuda HPC facility and Kanaad facility at the School of Physical Sciences, NISER. We are grateful to Jean-Yves Ollitrault, Björn Schenke, Chun Shen, Derek Teaney, Tribhuban Parida, and Rupam Samanta for insightful discussions on the new observable $v_0(p_T)$. We thank the ALICE Collaboration for making the $v_0(p_T)$ data publicly available. The Bayesian inference was performed using Python-based MCMC routines.

-
- [1] E. V. Shuryak, “Quark-Gluon Plasma and Hadronic Production of Leptons, Photons and Psions”, *Phys. Lett. B* **78** (1978) 150.
- [2] J. Cleymans, R. V. Gavai, and E. Suhonen, “Quarks and Gluons at High Temperatures and Densities”, *Phys. Rept.* **130** (1986) 217.
- [3] ALICE Collaboration, B. B. Abelev *et al.*, “Performance of the ALICE Experiment at the CERN LHC”, *Int. J. Mod. Phys. A* **29** (2014) 1430044, [arXiv:1402.4476 \[nucl-ex\]](https://arxiv.org/abs/1402.4476).
- [4] J.-Y. Ollitrault, “Relativistic hydrodynamics for heavy-ion collisions”, *Eur. J. Phys.* **29** (2008) 275–302, [arXiv:0708.2433 \[nucl-th\]](https://arxiv.org/abs/0708.2433).
- [5] J.-Y. Ollitrault, “Anisotropy as a signature of transverse collective flow”, *Phys. Rev. D* **46** (1992) 229–245.
- [6] S. Voloshin and Y. Zhang, “Flow study in relativistic nuclear collisions by Fourier expansion of Azimuthal particle distributions”, *Z. Phys. C* **70** (1996) 665–672, [arXiv:hep-ph/9407282](https://arxiv.org/abs/hep-ph/9407282).
- [7] W. Reisdorf and H. G. Ritter, “Collective flow in

- heavy-ion collisions”, *Ann. Rev. Nucl. Part. Sci.* **47** (1997) 663–709.
- [8] U. Heinz and R. Snellings, “Collective flow and viscosity in relativistic heavy-ion collisions”, *Ann. Rev. Nucl. Part. Sci.* **63** (2013) 123–151, [arXiv:1301.2826 \[nucl-th\]](#).
- [9] STAR Collaboration, K. H. Ackermann *et al.*, “Elliptic flow in Au + Au collisions at $\sqrt{s_{\text{NN}}} = 130$ GeV”, *Phys. Rev. Lett.* **86** (2001) 402–407, [arXiv:nucl-ex/0009011](#).
- [10] PHENIX Collaboration, K. Adcox *et al.*, “Formation of dense partonic matter in relativistic nucleus-nucleus collisions at RHIC: Experimental evaluation by the PHENIX collaboration”, *Nucl. Phys. A* **757** (2005) 184–283, [arXiv:nucl-ex/0410003](#).
- [11] ALICE Collaboration, K. Aamodt *et al.*, “Elliptic flow of charged particles in Pb-Pb collisions at 2.76 TeV”, *Phys. Rev. Lett.* **105** (2010) 252302, [arXiv:1011.3914 \[nucl-ex\]](#).
- [12] ALICE Collaboration, K. Aamodt *et al.*, “Higher harmonic anisotropic flow measurements of charged particles in Pb-Pb collisions at $\sqrt{s_{\text{NN}}}=2.76$ TeV”, *Phys. Rev. Lett.* **107** (2011) 032301, [arXiv:1105.3865 \[nucl-ex\]](#).
- [13] ATLAS Collaboration, G. Aad *et al.*, “Measurement of the azimuthal anisotropy for charged particle production in $\sqrt{s_{\text{NN}}} = 2.76$ TeV lead-lead collisions with the ATLAS detector”, *Phys. Rev. C* **86** (2012) 014907, [arXiv:1203.3087 \[hep-ex\]](#).
- [14] CMS Collaboration, S. Chatrchyan *et al.*, “Measurement of Higher-Order Harmonic Azimuthal Anisotropy in PbPb Collisions at $\sqrt{s_{\text{NN}}} = 2.76$ TeV”, *Phys. Rev. C* **89** (2014) 044906, [arXiv:1310.8651 \[nucl-ex\]](#).
- [15] ALICE Collaboration, J. Adam *et al.*, “Anisotropic flow of charged particles in Pb-Pb collisions at $\sqrt{s_{\text{NN}}} = 5.02$ TeV”, *Phys. Rev. Lett.* **116** (2016) 132302, [arXiv:1602.01119 \[nucl-ex\]](#).
- [16] ALICE Collaboration, S. Acharya *et al.*, “Skewness and kurtosis of mean transverse momentum fluctuations at the LHC energies”, *Phys. Lett. B* **850** (2024) 138541, [arXiv:2308.16217 \[nucl-ex\]](#).
- [17] ALICE Collaboration, S. Acharya *et al.*, “System size and energy dependence of the mean transverse momentum fluctuations at the LHC”, [arXiv:2411.09334 \[nucl-ex\]](#).
- [18] ATLAS Collaboration, G. Aad *et al.*, “Disentangling Sources of Momentum Fluctuations in Xe+Xe and Pb+Pb Collisions with the ATLAS Detector”, *Phys. Rev. Lett.* **133** (2024) 252301, [arXiv:2407.06413 \[nucl-ex\]](#).
- [19] P. Bożek and W. Broniowski, “Transverse momentum fluctuations in ultrarelativistic Pb + Pb and p + Pb collisions with “wounded” quarks”, *Phys. Rev. C* **96** (2017) 014904, [arXiv:1701.09105 \[nucl-th\]](#).
- [20] G. Giacalone, F. G. Gardim, J. Noronha-Hostler, and J.-Y. Ollitrault, “Skewness of mean transverse momentum fluctuations in heavy-ion collisions”, *Phys. Rev. C* **103** (2021) 024910, [arXiv:2004.09799 \[nucl-th\]](#).
- [21] R. Samanta, J. a. P. Picchetti, M. Luzum, and J.-Y. Ollitrault, “Non-Gaussian transverse momentum fluctuations from impact parameter fluctuations”, *Phys. Rev. C* **108** (2023) 024908, [arXiv:2306.09294 \[nucl-th\]](#).
- [22] E. Schnedermann, J. Sollfrank, and U. W. Heinz, “Thermal phenomenology of hadrons from 200-A/GeV S+S collisions”, *Phys. Rev. C* **48** (1993) 2462–2475, [arXiv:nucl-th/9307020](#).
- [23] STAR Collaboration, L. Adamczyk *et al.*, “Bulk Properties of the Medium Produced in Relativistic Heavy-Ion Collisions from the Beam Energy Scan Program”, *Phys. Rev. C* **96** (2017) 044904, [arXiv:1701.07065 \[nucl-ex\]](#).
- [24] ALICE Collaboration, S. Acharya *et al.*, “Production of charged pions, kaons, and (anti-)protons in Pb-Pb and inelastic pp collisions at $\sqrt{s_{\text{NN}}} = 5.02$ TeV”, *Phys. Rev. C* **101** (2020) 044907, [arXiv:1910.07678 \[nucl-ex\]](#).
- [25] B. Schenke, C. Shen, and D. Teaney, “Transverse momentum fluctuations and their correlation with elliptic flow in nuclear collision”, *Phys. Rev. C* **102** (2020) 034905, [arXiv:2004.00690 \[nucl-th\]](#).
- [26] T. Parida, R. Samanta, and J.-Y. Ollitrault, “Probing collectivity in heavy-ion collisions with fluctuations of the pT spectrum”, *Phys. Lett. B* **857** (2024) 138985, [arXiv:2407.17313 \[nucl-th\]](#).
- [27] ALICE Collaboration, S. Acharya *et al.*, “Long-range transverse momentum correlations and radial flow in Pb-Pb collisions at the LHC”, [arXiv:2504.04796 \[nucl-ex\]](#).
- [28] ATLAS Collaboration, G. Aad *et al.*, “Evidence for the collective nature of radial flow in Pb+Pb collisions with the ATLAS detector”, [arXiv:2503.24125 \[nucl-ex\]](#).
- [29] CMS Collaboration, V. Khachatryan *et al.*, “Observation of Long-Range Near-Side Angular Correlations in Proton-Proton Collisions at the LHC”, *JHEP* **09** (2010) 091, [arXiv:1009.4122 \[hep-ex\]](#).
- [30] CMS Collaboration, S. Chatrchyan *et al.*, “Observation of Long-Range Near-Side Angular Correlations in Proton-Lead Collisions at the LHC”, *Phys. Lett. B* **718** (2013) 795–814, [arXiv:1210.5482 \[nucl-ex\]](#).